Thermochimica Acta 500 (2010) 21–29

Contents lists available at ScienceDirect

Thermochimica Acta

journal homepage: www.elsevier.com/locate/tca

In situ prepared PET nanocomposites: Effect of organically modified montmorillonite and fumed silica nanoparticles on PET physical properties and thermal degradation kinetics

A.A. Vassiliou [a], K. Chrissafis [b], D.N. Bikiaris [a,*]

[a] Laboratory of Organic Chemical Technology, Department of Chemistry, Aristotle University of Thessaloniki, GR-541 24 Thessaloniki, Macedonia, Greece
[b] Solid State Physics Section, Physics Department, Aristotle University of Thessaloniki, GR-541 24 Thessaloniki, Macedonia, Greece

ARTICLE INFO

Article history:
Received 2 October 2009
Received in revised form 5 December 2009
Accepted 10 December 2009
Available online 23 December 2009

Keywords:
Poly(ethylene terephthalate)
Montmorillonite
Fumed silica
Nanocomposites
Thermal degradation
Activation energy

ABSTRACT

In the present study a series of PET nanocomposites were prepared by in situ polymerization using different amounts of organically modified montmorillonite (OMMT) with a triphenylphosphine compound and fumed silica nanoparticles (SiO_2). As verified by TEM micrographs, the dispersion of both nanoparticles into the PET matrix was homogeneous while montmorillonite was dispersed in the exfoliated form. The intrinsic viscosities of the prepared nanocomposites were affected by the addition of the nanoparticles and in both cases a slight increase was observed. Tensile strength was also increased by increasing nanoparticles content while both types of nanoparticles act as nucleating agents, enhancing the crystallization rates of PET. From the thermogravimetric curves it was concluded that PET and the samples with different nanoparticles presented good thermostability, since no remarkable mass loss occurred up to 320 °C (<0.5%). The activation energy (E) of degradation of the studied samples was estimated using the Ozawa, Flynn and Wall (OFW) method. Pure PET had an E = 223.5 kJ/mol while the activation energy of PET/SiO_2 2 wt.% nanocomposites was almost identical (222.1 kJ/mol). However, PET/OMMT 2 wt.% nanocomposites exhibited a higher activation energy (228.3 kJ/mol), indicating that OMMT incurred a stabilizing effect upon the decomposition of the matrix. The form of the conversion function for all the studied samples obtained by fitting was the mechanism of n^{th}-order auto-catalysis.

1. Introduction

Poly(ethylene terephthalate) (PET) is of major industrial importance due to its low cost and high performance (since it has high glass transition and melting temperatures) as well as good physical properties. It has been found a variety of applications such as in textile fibers, films, bottle containers, food packaging materials, engineering plastics in automobiles, electronics, etc. Its properties depend mainly on the degree of orientation of the polymer chains and the degree of crystallinity. Furthermore, in recent years there is an increasing interest for the preparation of PET nanocomposites, due to their enhanced mechanical, thermal and gas barrier properties, for many applications [1–4]. However, only few papers are reported concerning the study of thermal stability properties of PET nanocomposites. Zheng et al. [5] studied PET with different silica content of 1, 3, 5 wt.% using non-isothermal measurements under nitrogen gas. They used Friedman method to investigate the activation energy. The average calculated values of activation energy were: 178, 198, 215, 214 for pure PET and the different PET/silica nanocomposites. Wang et al. [6] studied the thermal stability and degradation of PET/montmorillonite (MMT) nanocomposites with TGA under N_2 atmosphere. They showed that the onset temperature of degradation and the temperature at maximum mass loss rate were increased significantly by adding MMT. When MMT content was in the low range (<5%), the observed thermal stability behavior of PET/MMT was decided by both MMT content and its dispersion quality.

TGA is one of the most widely used techniques in the study of the thermal decomposition of polymers [7]. In absence of prior information about real kinetic mechanism the reaction model can be chosen from a set of well-known reaction models to fit experimental data, usually done in model-fitting techniques. In recent years there is an increasing interest for the precise determination of the model reaction and the activation energy of PET. Yang et al. [8] using the DTG curve fitting method on non-isothermal measurements under N_2 atmosphere calculated the activation energy (E = 242 kJ/mol) using first-order reaction model. Holland and Hay [9] studied the thermal degradation of PET with non-isothermal and isothermal thermogravimetry under Ar atmosphere. In this study first-order reaction was used and the value

* Corresponding author. Tel.: +30 2310 997812; fax: +30 2310 997667.
E-mail address: dbic@chem.auth.gr (D.N. Bikiaris).

0040-6031/$ – see front matter © 2009 Elsevier B.V. All rights reserved.
doi:10.1016/j.tca.2009.12.005

of activation energy was determined from isothermal measurements ($E = 220 \pm 10$ kJ/mol). Using non-isothermal measurements he showed that the activation energy, calculated with Ozawa's method, varied with mass conversion, having an average value of 180 ± 10 kJ/mol. The values of E calculated with Coats and Redfern's method showed enough scattering – the values varied between 250 and 290 kJ/mol – and by Friedman's method was found to be $E = 170 \pm 10$ kJ/mol. Saha and Ghoshal [10] studied the thermal degradation of PET using soft drink bottles. The calculated values of E was 162.1 and 210.6 kJ/mol using the ASTM E698 method with first reaction order and 322.3 and 339 kJ/mol using n^{th}-order model for two different samples. Also, Saha et al. [11] used the Vyazovkin model-free approach to study non-isothermal decomposition kinetics of waste PET samples using various temperature integral approximations, such as Coats and Redfern, Gorbachev, and Agrawal and Sivasubramanian. Their results showed that the activation energy was a weak but increasing function of mass conversion in case of non-isothermal decomposition and strong and decreasing function of conversion in case of isothermal decomposition.

In the present study PET nanocomposites containing different amounts of organically modified montmorillonite (OMMT) and fumed silica nanoparticles (SiO_2) were prepared by in situ polymerization and studied.

The objective of this study was the characterization of PET nanocomposites and to study the effect of different types of nanoparticles on PET properties as well as its thermal stability. Particularly, kinetics and the mechanism of thermal decomposition were studied, while the activation energy of the process was also calculated. Furthermore, since neat MMT cannot be sufficiently dispersed into the polymer matrix, in the present study organically modified montmorillonite (OMMT) with a triphenylphosphine compound was used. The modification was achieved using a thermally stable modifier.

2. Experimental

2.1. Materials

Dimethyl terephthalate (DMT) (99%), anhydrous 1,2-ethanediol (EG) (99%), antimony trioxide (Sb_2O_3) (98%) and triphenylphosphate (TPP) (95%) were obtained from Fluka. Zinc acetate [$(CH_3CO_2)_2Zn$] (99.99%) was purchased from Sigma–Aldrich. Fumed silica nanoparticles (SiO_2) under the trade name AEROSIL® 200 were supplied by Degussa AG (currently Evonik Industries) (Hanau, Germany). The nanoparticles had an average primary particle size of 12 nm, a specific surface area of $200\ m^2\ g^{-1}$ and a SiO_2 content >99.8%. Pristine montmorillonite [$Na_x(Al_{4-x}Mg_x)Si_8O_{20}(OH)_4$, $0.5 \geq x \geq 1.3$] under the trade name Cloisite Na^+ was obtained from Southern Clay Products Inc. (Gonzales, TX, USA). It had a Cation Exchange Capacity (CEC) of 92 mequiv./100 g. Triphenylphosphine ($(C_6H_5)_3P$) (≥95.0%) and 1-chlorohexadecane ($CH_3(CH_2)_{15}Cl$) (≥97.0%) were supplied from Sigma–Aldrich. All other materials and solvents used for the analytical methods were of analytical grade.

2.2. Modification of montmorillonite

To prepare the organic modifier for the pure montmorillonite 1-chlorohexadecane and triphenylphosphine were added in a round bottom flask at a molar ratio of 1:1. The mixture was heated in an inert atmosphere (argon) at 100 °C for 2 h under constant mechanical stirring. The final viscous product was extensively washed with petroleum ether and dried at 50 °C for 24 h. For the modification of the neat montmorillonite 25 g of Cloisite-Na^+ were added in 1 L of distilled water and the suspension was stirred for 24 h. The suspension was then cooled (0–5 °C) and 30 mmol of the aforementioned synthesized organic modifier dissolved in 100 mL of distilled water was added drop-wise. After 3 h of stirring at 0–5 °C, the white precipitate was removed by filtration, washed with distilled water until no chloride ions were detectable from an aqueous solution of $AgNO_3$. Subsequently, the sample was left to dry at room temperature under vacuum for 24 h, and then it was suspended in petroleum ether under constant stirring for 3 h. The sample was removed by filtration and washed again with additional petroleum ether. Finally, the organically modified montmorillonite, MMT-$Ph_3P^+C_{16}Cl$ (OMMT), was dried at 70 °C for 24 h.

2.3. In situ preparation of PET/OMMT and PET/SiO_2 nanocomposites

Nanocomposites of poly(ethylene terephthalate) were prepared in situ by the two-stage melt polycondensation of DMT and EG in a glass batch reactor. The nanoparticles were dried in vacuum at 120 °C for 24 h. Appropriate amount of filler was dispersed in EG by ultrasonic vibration (50 W) and intense stirring with a magnetic stirrer (300 rpm) for 10 min prior to polymerization. Zinc acetate was added (1×10^{-3} mol/mol DMT) and DMT at a molar ratio of DMT/EG = 1/2.2. The mixture was de-aired and purged with argon tree times. Subsequently, it was heated at 190 °C for 1 h, under constant mechanical stirring (500 rpm). The methanol produced by the transesterification reaction was removed from the mixture by distillation and collected in a graduated cylinder. The temperature was raised to 230 °C and the reaction continued for a further 2 h, were the complete removal of the anticipated produced methanol took place.

During the second stage, under an argon atmosphere, the polycondensation catalyst (Sb_2O_3, 250 ppm) and TPP (0.03 wt.% DMT) as thermal stabilizer, dispersed in a small amount of EG, were added in the mixture. TPP is known to prevent side reactions such as etherification and thermal decomposition. Afterwards, vacuum was applied (~5 Pa) slowly, over a period of 15 min, to avoid excessive foaming and to minimize oligomer sublimation, which is a potential problem during the melt polycondensation. The temperature was raised to 280 °C and the reaction ensued for 2 h. When the polycondensation reaction was completed, the reaction tube was broken to remove the product out of the flask. All polyester samples, after the glass particles were removed with a grinder, were grounded in a mill, sieved, washed with methanol and dried at 110 °C for 12 h.

Different amounts of filler were added at the beginning of the transesterification reaction. PET/OMMT and PET/SiO_2 nanocomposites were prepared containing 0.5, 1.0 and 2.0 wt.% of nanoparticles.

2.4. Intrinsic viscosity

Intrinsic viscosity [η] measurements on the isolated polymers were performed using an Ubbelohde viscometer cap. Ic at 25 °C in phenol/tetrachloroethane 60/40 w/w at a solution concentration of 1 wt.%. The solutions were filtered through a disposable membrane filter 0.2 μm (Teflon) prior to the measurement.

The number-average molecular weight $\bar{M}_n$ of the samples was calculated from intrinsic viscosity [η] values, using the Berkowitz equation [12]:

$$\bar{M}_n = 3.29 \times 10^4 \times [\eta]^{1.54} \quad (1)$$

Table 1
Molecular weight, thermal and mechanical properties of the prepared PET nanocomposites.

Sample	$[\eta]$ (dL/g)	$\bar{M}_n$ (g/mol)	T_g (°C)	T_{cc} (°C)	T_m (°C)	ΔH_m (J/mol)	Tensile strength (MPa)
PET	0.63	16 000	82.3	161.7	250.8	32.2	32 ± 1.3
PET + 0.5 wt.% SiO_2	0.74	20 500	82.3	153.2	250.9	31.8	36 ± 1.9
PET + 1.0 wt.% SiO_2	0.70	19 200	83.4	143.2	251.5	32.3	40 ± 1.6
PET + 2.0 wt.% SiO_2	0.69	18 500	83.6	128.5	253.6	31.5	45 ± 2.2
PET + 0.5 wt.% OMMT	0.63	16 000	82.3	152.6	255.6	32.4	33 ± 1.5
PET + 1.0 wt.% OMMT	0.71	19 500	82.3	148.4	256.1	32.5	35 ± 2.1
PET + 2.0 wt.% OMMT	0.82	24 000	82.8	142.1	256.2	32.6	39 ± 1.9

2.5. Differential scanning calorimeter (DSC)

The thermal measurements were carried out using a Setaram DSC141 unit. Temperature and energy calibrations of the instrument were performed at different heating rates, using the melting temperatures and melting enthalpies of high-purity zinc, tin and indium supplied with the instrument. The samples used were in powder form and weighed about 7 mg. They were crimped in aluminum crucibles and an empty aluminum crucible was used as reference. The samples were heated to 280 °C at a scanning rate of 20 °C/min, remained at that temperature for 3 min, then they quenched rapidly in cold water in order to be obtained in the amorphous state and rescanned again to 280 °C at the same heating rate. A constant nitrogen flow was maintained to provide a constant thermal blanket within the DSC cell, thus eliminating thermal gradients and ensuring the validity of the applied calibration standard from sample to sample. From the recorded thermograms the glass transition temperature (T_g), cold-crystallization temperature (T_{cc}), melting point (T_m) and heat of fusion (ΔH_m) were measured.

2.6. Transmission electron microscopy

Electron diffraction (ED) and transmission electron microscopy (TEM) observations were made on ultra thin film samples of the various nanocomposites prepared by an ultra-microtome. These thin films were deposited on copper grids. ED patterns and TEM micrographs were obtained using a JEOL 120 CX microscope operating at 120 kV. To avoid the destruction of the films after exposure to the electron irradiation, an adequate sample preparation is required, thus, the thin films were coated with carbon black.

2.7. X-ray diffraction patterns (XRD)

X-ray diffraction measurements of the samples were performed by an automated Philips PW 1050 powder diffractometer with Bragg-Brentano geometry (θ–2θ), using Cu K_a radiation (λ = 0.15406 nm) over the range 2θ range from 5° to 55° at steps of 0.05° and counting time of 5 s at room temperature.

2.8. Mechanical properties

Measurements of tensile mechanical properties of the prepared nanocomposites were performed on an Instron 3344 dynamometer, in accordance with ASTM D638, using a crosshead speed of 50 mm/min. Relative thin sheets of about 150 ± 10 μm were prepared using an Otto Weber, Type PW 30 hydraulic press connected with an Omron E5AX Temperature Controller, at a temperature of 270 ± 5 °C. The moulds were rapidly cooled by immersing them in water at 20 °C. From these sheets, dumb-bell-shaped tensile test specimens (central portions 5 mm × 0.5 mm thick, 22 mm gauge length) were cut in a Wallace cutting press and conditioned at 25 °C and 55–60% relative humidity for 48 h. The values of tensile strength at the break point were determined. At least five specimens were tested for each sample and the average values, together with the standard deviations, are reported.

2.9. Thermogravimetric analysis

Thermogravimetric (TG) analysis was carried out with a SETARAM SETSYS TG-DTA 1750 °C. Samples (5.5 ± 0.2 mg) were placed in alumina crucibles. An empty alumina crucible was used as reference. Samples were heated from ambient temperature to 600 °C in a 50 mL/min flow of N_2. Heating rates of 5, 10, 15 and 20 °C/min were used and continuous recordings of sample temperature, sample weight, its first derivative and heat flow were taken.

3. Results and discussion

3.1. Characterization of PET nanocomposites

In most of the reported studies in the literature the nanocomposites were prepared using the solvent mixing or melt mixing methods, since these are very easy methods and economical. However, the main drawback of these methods is the poor dispersion of the nanoparticles into the polymer matrix. In the present study PET nanocomposites were prepared in situ through polymerization of PET by the two-stage melt polycondensation reaction with the nanoparticles added at the beginning of polymerization. Since both SiO_2 and OMMT nanoparticles have a lot of surface reactive groups it was believed that these could interact with the –COOH or –OH end groups of PET and a better dispersion of the nanoparticles would be achieved. The intrinsic viscosity of pure PET that was prepared according to the described experimental procedure was 0.63 dL/g, corresponding to a molecular weight of 16 000 g/mol (Table 1).

The presence of the different types of nanoparticles in the polymerization mixture affected the reaction, leading to variations of the final intrinsic viscosities of the prepared nanocomposites. As shown in Table 1, the intrinsic viscosity was in all nanocomposites higher compared to pure PET. Such an increase was also found in our previous studies by adding SiO_2 nanoparticles in poly(ε-caprolactone) [13] and poly(butylene succinate) [14]. SiO_2 nanoparticles contain surface silanol groups (≡Si–OH) which due to their weak acidic nature can interact with the hydroxyl end groups of polyesters. The possibility of such a reaction between the surface silanol groups of fumed silica nanoparticles and the hydroxyl end groups of the polymer were first hinted in one of our previous study in nanocomposites consisted by poly(ethylene terephthalate) and fumed silica nanoparticles [15]. More substantiation was subsequently obtained by measurements using solid-state ^{29}Si NMR and FTIR on nanocomposites of fumed silica with PET [16] and PBSu, indicating the possibility of covalent bonding between the fumed silica nanoparticles and the PBSu polymer backbone chain [17]. Thus, the nanoparticles could act as multifunctional additives, increasing the molecular weight of the polymer. However, as was found from our previous studies, at higher contents, due to the extended reactions, branched and crosslinked macromolecules are formed reducing the molecular weight [15,18].

In the case of PET/OMMT nanocomposites there is a continuous increase of molecular weight of PET as the OMMT content increases (Table 1). This effect could be attributed to the better thermal stabil-

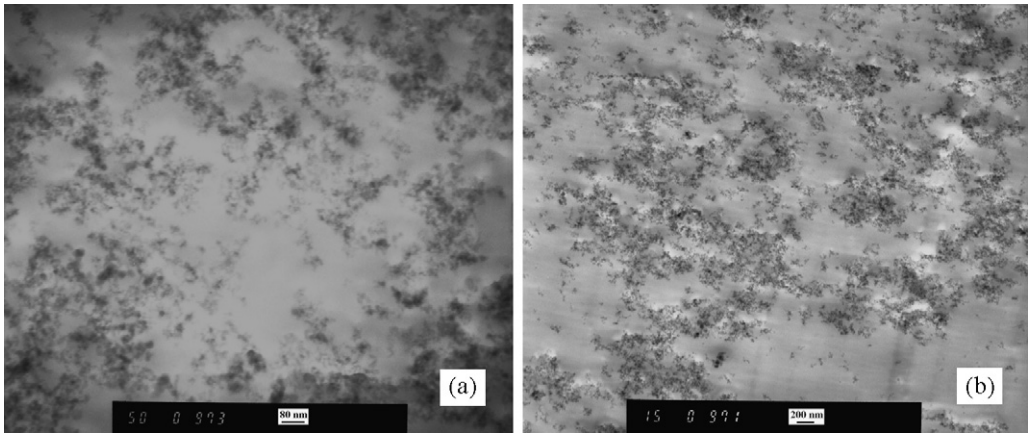

Fig. 1. TEM micrographs of PET/SiO_2 nanocomposites containing (a) 1.0 wt.% and (b) 2.0 wt.% of SiO_2 nanoparticles.

ity of PET and the suppressions of thermal decomposition reactions that took place during PET synthesis. Also, a possible increase of the heat conductivity of the polymerization mixture, due to the presence of the inorganic filler, could also contribute to the observed trend.

The dispersion of PET nanocomposites containing SiO_2 nanoparticles was studied by TEM micrographs (Fig. 1). As can be seen, the dispersion was very fine, even at the highest concentration of 2 wt.% of SiO_2. Furthermore, it was clear that very small aggregates (<200 nm), which are almost inevitable for such nanoparticles, coexist with single nanoparticles in the samples.

To investigate the degree of dispersion of OMMT in the PET matrix X-ray diffraction patterns and TEM micrographs were used complementary. For the pristine MMT, a strong X-ray diffraction peak at $2\theta = 7.58^\circ$ (Fig. 2) was caused by the diffraction of the (0 0 1) crystal surface of layered silicates, equaling a d-spacing of about 11–12 Å. After treatment with the triphenylphosphine compound this peak was almost disappeared and a new was recorded at $2\theta = 2.39^\circ$, indicating that the distance between the silicate layers was increased. As shown in Fig. 2, at the concentrations of 1 and 2 wt.% OMMT the peak corresponding to the crystallographic plane (0 0 1) ($d_{(0\,0\,1)}$) of OMMT (2.39°) does not appear. This means that a fine dispersion of the montmorillonite plates into the PET matrix has been achieved, since with the help of the organic modifier the polymer macromolecules were able to penetrate between the montmorillonite layers increasing the distance between them and ultimately leading to their separation. Therefore, the montmorillonite was dispersed in the exfoliated form into the PET matrix indicating the effectiveness of triphenylphosphine compound. It

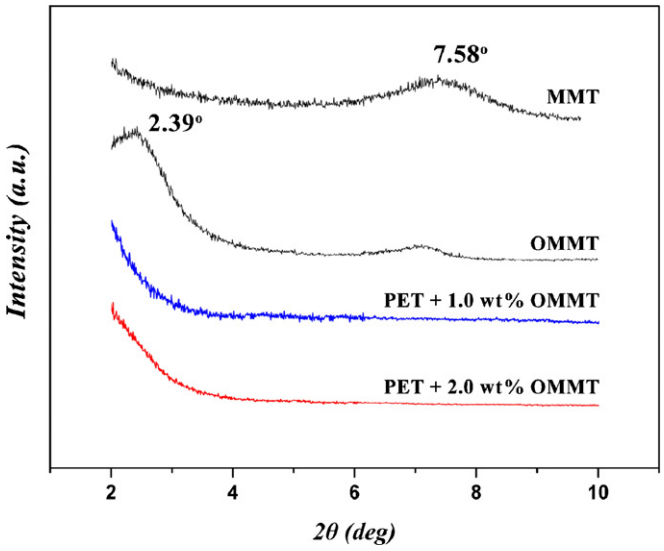

Fig. 2. XRD patterns of PET/OMMT nanocomposites.

should be noted that the small peak present at $2\theta = 7^\circ$ in the diffraction pattern of OMMT was, after calculations, confirmed to be due to the crystallographic plane (0 0 2) ($d_{(0\,0\,2)}$) of montmorillonite.

The above became more self-evident in the TEM micrographs of these samples (Fig. 3). For concentrations up to 2 wt.% the layers of montmorillonite were mainly separated and dispersed finely in

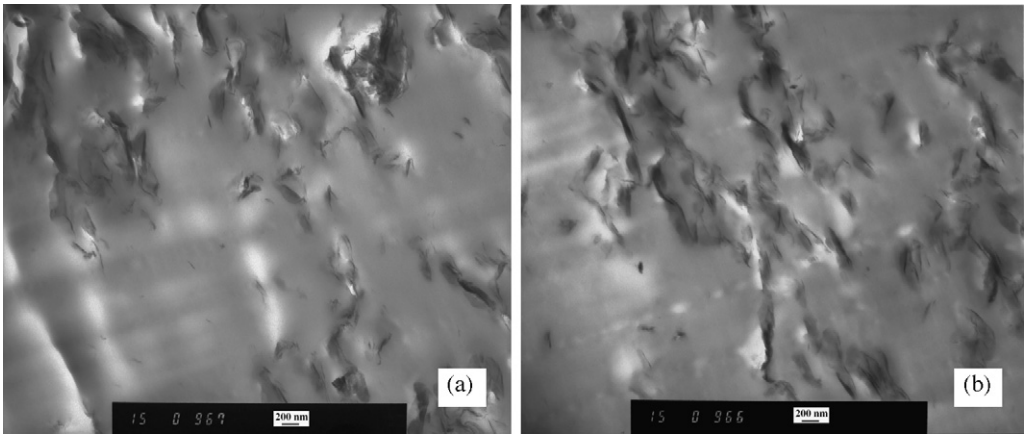

Fig. 3. TEM micrographs of PET/OMMT nanocomposites containing (a) 1.0 wt.% and (b) 2.0 wt.% of OMMT nanoparticles.

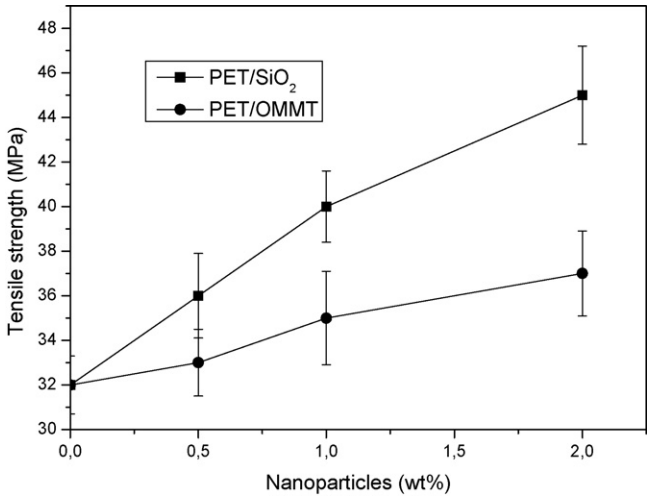

Fig. 4. Tensile strength of PET nanocomposites containing different amounts of SiO_2 and OMMT nanoparticles.

the polymer matrix. However, some small intercalated aggregates could also be observed in the samples, but for concentration even up to 2 wt.% these were of low magnitude. Considering, furthermore, the relatively very small concentration of the nanoparticles in the sample it becomes evident why these intercalated structures were not detected with the XRD method.

The variations of molecular weights and the fine dispersion of nanoparticles, as verified above, affected the mechanical properties of the nanocomposites [19]. Neat PET is very brittle and breaks before yield point with tensile strength 32 ± 1.3 MPa (Fig. 4). This brittleness remains also in all nanocomposites. However, there are substantial improvements in their mechanical properties. In the case of PET/SiO_2 nanocomposites tensile strength increases continuously by increasing SiO_2 content. Taking into account that molecular weight remains the same in all nanocomposites, this increase should be attributed to the produced branched macromolecules [15]. Such behavior was also found in our previous study by using multifunctional co-monomer as crosslinking additive [20]. An additional proof about this claim is that PET/OMMT nanocomposites have lower tensile strength, compared with PET/SiO_2 nanocomposites. In this case it is very difficult branched macromolecules to form and the recorded increase in tensile strength should be attributed to the reinforcement effect of nanoclay. This is a substantial improvement in tensile strength compared with reported values in literature, where a decrease in tensile strength was observed when clays modified with quaternary ammoniums were used [21]. These modifiers are reducing the molecular weight of PET, while the used in our paper based on triphenylphosphine has not such effect.

Branched macromolecules can also affect the thermal properties of PET nanocomposites. As can be seen from Table 1 the glass transition temperatures of PET/SiO_2 nanocomposites tend to shift to higher temperatures by increasing SiO_2 content. These results are in agreement with those reported in literature [22–24]. As mentioned, usually the T_g of a polymeric matrix tends to increase with the addition of nanoparticles, due to the interactions between the polymer chains and the nanoparticles and to the reduction of macromolecular chain mobility at the zone surrounding the nanoparticles [22–24]. This transition zone exhibits higher modulus and T_g, both of which are gradually reduced with increasing distance from the filler surface. However, in the case of PET/OMMT nanocomposites the differences in T_g values are negligible and thus the recorded increase in PET/SiO_2 nanocomposites should be attributed mainly to the formed branched macromolecules [20,25].

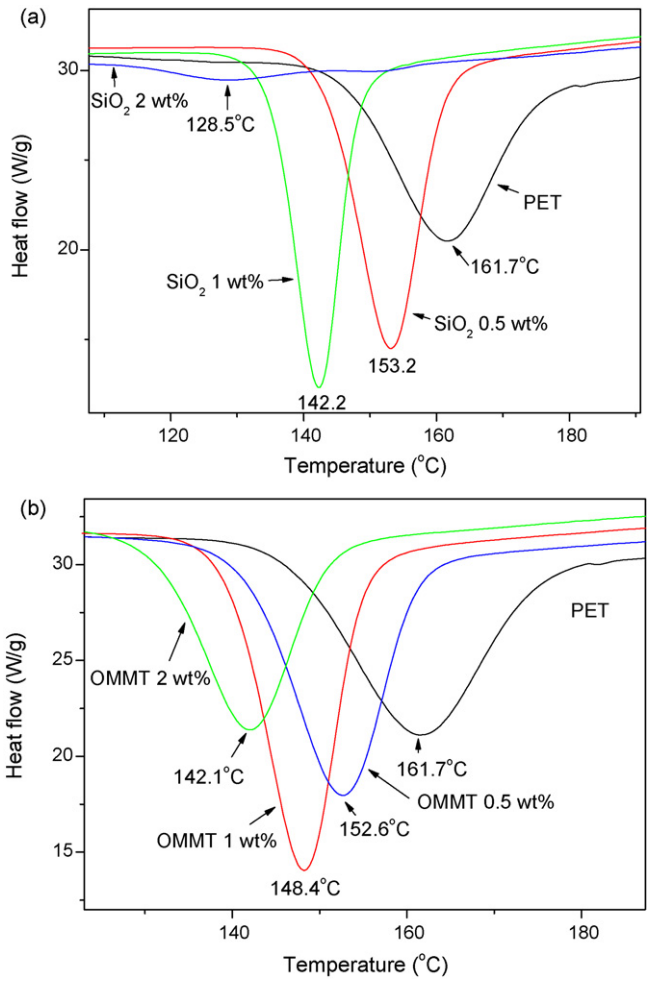

Fig. 5. Cold-crystallization temperatures of (a) PET/SiO_2 nanocomposites and (b) PET/OMMT nanocomposites containing different content of nanoparticles.

In the case of PET/OMMT despite good dispersion of nanoparticles in the PET matrix, there is no strong interaction so that the polymer chains experience no significant nanoconfinement, i.e., no significant restriction in their mobility.

The melting point of PET was recorded at 250.8 °C while in the nanocomposites a slight increase was found by increasing the amount of SiO_2 and OMMT nanoparticles. This could be attributed to a nucleation effect by the nanoparticles, increasing the degree of crystallinity of PET. However, as can be seen from the heat of fusions, the effect of the nanoparticles on the degree of crystallinity seems to be negligible. The nucleation effect of SiO_2 and OMMT nanoparticles can be seen more characteristically from cold-crystallization temperature (T_{cc}) measurements. For cold-crystallization behavior, the T_{cc} values of nanocomposites are lower than that of pure PET (Fig. 5). For example, T_{cc} is decreased from 161.2 °C of neat PET to 142.2 °C of PET containing 1 wt.% SiO_2 or to 148.4 °C of PET containing 1 wt.% OMMT. The decrease of T_{cc} means that the cold-crystallization of PET in nanocomposites becomes easier than in neat PET. This lower cold-crystallization temperature can be attributed to SiO_2 and OMMT nanoparticles which acting as nucleating agents is enhancing the crystallization of PET macromolecules. This is probably due to the fact that nanoparticles have higher surface area in contact with semicrystalline polymer matrices and thus induce a heterogeneous nucleation effect [26–30]. Comparing the differences in cold-crystallization temperatures of PET nanocomposites it can be seen that the recorded values for PET/SiO_2 nanocomposites are lower than the corresponding of

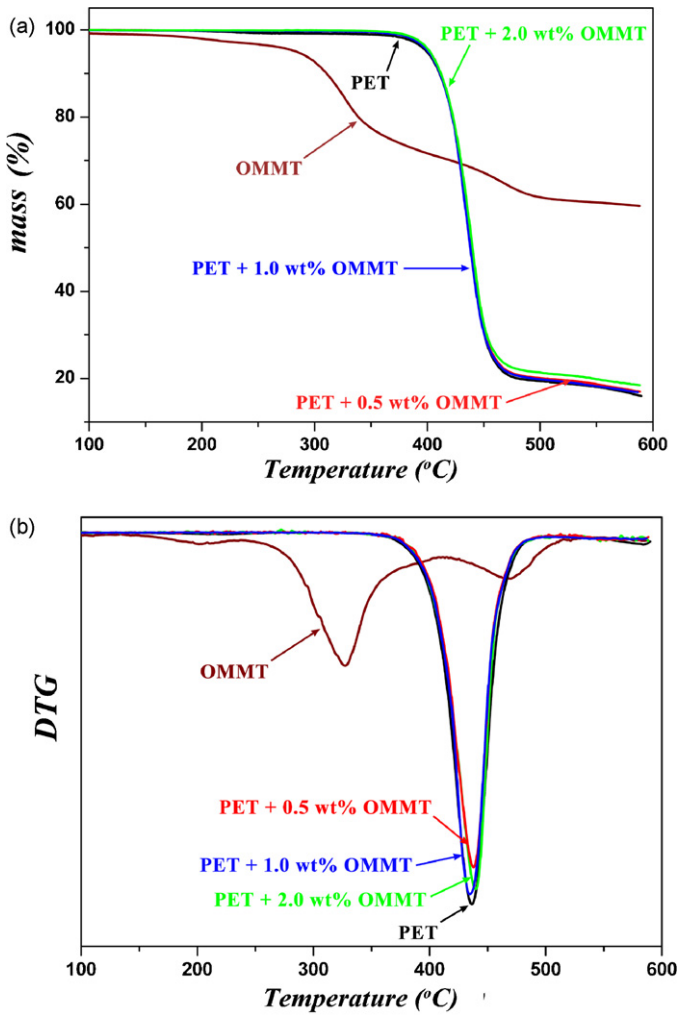

Fig. 6. (a) Mass (%) versus temperature and (b) derivative mass (DTG) versus temperature at a heating rate of $\beta = 10\,^{\circ}$C/min for PET nanocomposites with OMMT.

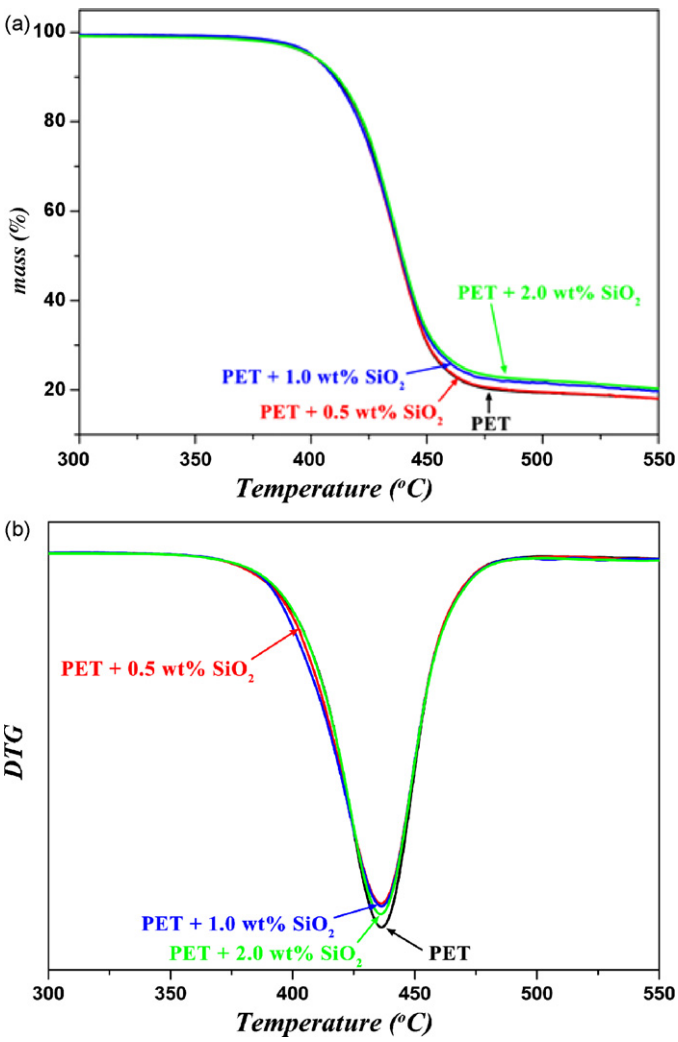

Fig. 7. (a) Mass (%) versus temperature and (b) derivative mass (DTG) versus temperature at a heating rate of $\beta = 10\,^{\circ}$C/min for PET nanocomposites with SiO_2.

PET/OMMT nanocomposites. This indicates that maybe SiO_2 has a higher nucleating effect than OMMT. One possible reason for such behavior is that SiO_2 interacts with PET matrix forming covalent bonds [15] and a second reason is that maybe SiO_2 has a finer dispersion into PET matrix than OMMT. Thus, the available surface in contact with PET macromolecules may be higher.

3.2. Thermogravimetric analysis

Thermal degradation of PET with different concentrations of OMMT and SiO_2 was studied by determining its mass during heating. In Figs. 6 and 7 the mass (%) and the derivative mass (DTG) curves of all studied samples are presented, at a heating rate of 10 °C/min. It is well known that when montmorillonite is used as an additive, in order to achieve a finer dispersion into the polymer matrix it is usually modified with organic additives, mainly with ammonium salts [19]. However, montmorillonites modified with such organic additives these are not particularly stable [31] and cannot be used in the case of PET, which has a melting point and processing temperature higher than 250 °C. Furthermore, the reactive ammonium groups can incur degradation of PET though aminolysis reactions. For the aforementioned reasons, in the present study a thermally stable modifier was prepared. In particular a phosphonium salt, which are known to be thermally stable and are characterized by less toxicity compared to their ammonium counterparts [31]. Moreover, the thermal stabilizing effect of phosphoric compounds on polymers is very well established and documented. As can be seen from its thermogravimetric curve the decomposition of OMMT took place at three different stages. At first stage, a small mass loss (less than 5 wt.%) gradually occurred up to 300 °C, at which mainly the absorbed water of montmorillonite was lost. The highest rate of the second decomposition stage took place at about 325 °C, which is a lot higher compared to the temperature at which PET is synthesized, while the third decomposition stage took place at a temperature of 470 °C. This confirmed that a thermally stable organically modified montmorillonite was prepared.

Concerning the nanocomposites, from the thermogravimetric curves it can be seen that PET and the samples with different nanoparticles presented a good thermostability. No remarkable mass loss occurred up until 330 °C (<0.4%) for PET-OMMT (Fig. 6) and 320 °C (<0.5%) for PET-SiO_2 (Fig. 7). As seen from the peak of the first derivative, the temperature at which the PET decomposition rate was highest was at $T_p = 436.4\,^{\circ}$C, for a heating rate of 10 °C/min. The same temperature was at $T_p = 437.8 \pm 1.3\,^{\circ}$C for PET-OMMT and at $T_p = 436.2 \pm 0.2\,^{\circ}$C for PET-$SiO_2$. The shape of the mass curve was the same in all samples while the above mentioned temperatures were slightly affected by the nanoparticles' amount. The recorded differences as seen from the first derivative curve were in the area of experimental error. Thus, in the case of PET/OMMT nanocomposites it could be said that the addition of OMMT caused a stabilization effect, while in the case of PET/SiO_2 nanocompos-

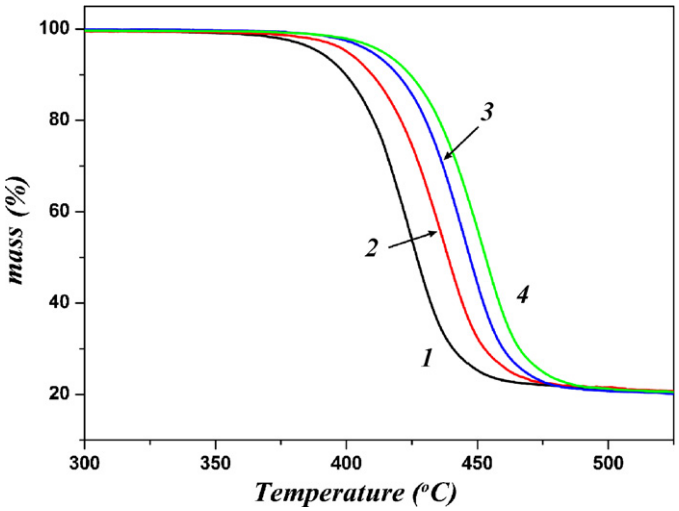

Fig. 8. Mass (%) curves at different heating rates β for PET containing 2.0 wt.% SiO_2. (1) $\beta = 5\,K\,min^{-1}$, (2) $\beta = 10\,K\,min^{-1}$, (3) $\beta = 15\,K\,min^{-1}$, (4) $\beta = 20\,K\,min^{-1}$.

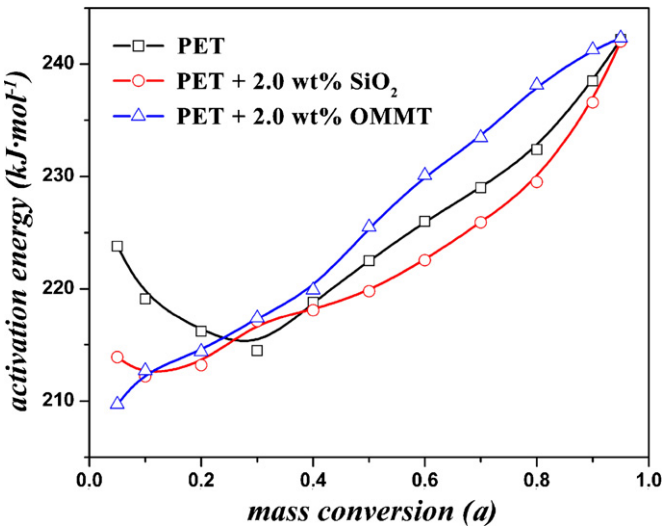

Fig. 9. Dependence of the activation energy (E) on the degree of the conversion (α) of the mass loss, as calculated with the OFW method for the different samples (lines are drawn to guide the eye).

ites the effect of SiO_2 on PET's thermal degradation was negligible. These differences could be attributed to the different shapes and magnitude of the used nanoparticles. Montomorillonite nanoparticles have a plate-like shape exhibiting high length, while silica nanoparticles have a spherical shape. Thus, OMMT nanoparticles have a better shielding effect and the evolved gases during thermal decomposition are difficultly liberated from the matrix.

In order for the degradation mechanism of PET with OMMT and SiO_2 to be analysed more thoroughly, it was important that the kinetic parameters (activation energy E and pre-exponential factor A) and conversion function $f(\alpha)$ were evaluated. The relationship between kinetic parameters and conversion (α) can be found by using the mass curves recorded in TG dynamic thermograms. Since the effect of small nanoparticles amounts seems to be very small, only nanocomposites containing the highest nanoparticles content were studied. The thermogravimetric curves of PET containing 2.0 wt.% SiO_2 heated under N_2 at different heating rates are shown in Fig. 8, as an example, at the temperature range just above the melting point up to 550 °C. It was clear that the peak temperature, T_p, shifted to higher values with increasing heating rate.

The activation energy E can be calculated by various methods. One of them is the isoconversional method of Ozawa, Flynn and Wall (OFW) [32,33]. It is, in fact, a "model-free" method which assumes that the conversion function $f(\alpha)$ does not change with the alteration of the heating rate for all values of the fractional extent of reaction α. It involves the measuring of the temperatures corresponding to fixed values of the degree of the mass conversion α from experiments at different heating rates β using the following equation:

$$\ln\ \beta = \ln\left[\frac{Af(\alpha)}{da/dT}\right] - \frac{E}{RT} \qquad (2)$$

Therefore, plotting $\ln(\beta)$ against $1/T$ according to Eq. (2) should give straight lines, the slope of which is directly proportional to the activation energy ($-E/R$). If the determined activation energy is the same for the various values of α, the existence of a single-step reaction can be concluded with certainty. On the contrary, a change in E with increasing degree of conversion is an indication of a complex reaction mechanism that invalidates the separation of variables involved in the OFW analysis [34]. These complications are serious, especially in the case where the total reaction involves competitive reaction mechanisms.

In order to calculate the activation energy of PET nanocomposites their mass curves were used. In Fig. 9 the dependence of the activation energy (E) versus conversion α for PET, PET containing 2.0 wt.% OMMT and PET containing 2.0 wt.% SiO_2 can be seen comparatively. It can be seen that OMMT improves slightly the thermal stability of PET but SiO_2 not, as was already discussed before. This is very important since in literature poor improvement in PET/clay nanocomposites was reported [35,36] indicating that the prepared organic modifier has not a negative effect in thermal stability of PET. The poor improvements in thermal stability of the PET/SiO_2 nanocomposites prepared hereby probably arise from the low inorganic content used, conjugated to the obtaining of intercalated structures rather than exfoliated structures. These results are in agreement with a previous paper concerning the enhancement thermal stability of polystyrene by using clay nanoparticles [24]. It was reported that the presence of intercalated clay nanoparticles has a stronger stabilizing effect in the early stages. This is because the plate nanoparticles form a more effective diffusion barrier and thus the diffusion of formed gasses during thermal degradation of PET is hindered. Furthermore, from our previous study on PCL nanocomposites it was found by TGA analysis that organically modified montmorillonite and fumed silica nanoparticles accelerated the decomposition of PCL due to respective aminolysis and hydrolytic reactions that the surface reactive groups these materials can induce [18]. On the other hand, carbon nanotubes and unmodified montmorillonite decelerated the thermal degradation of PCL due to a shielding effect.

The reaction mechanism of polymer decomposition is a very complex radical chain mechanism, including initiation, propagation and termination reactions. As it is well known, two main types of reaction models are generally applied on the thermal degradation of polymers: the n^{th}-order model with only one parameter and the first-order model. Other models have also been used occasionally, but they are complex models containing several fitting parameters.

To determine the conversion function $f(\alpha)$ we used a method referred to as the "model-fitting method" [37–41]. This method, that does not assume the knowledge of E and $f(\alpha)$ in advance, was applied simultaneously on the experimental data taken at the heating rates $\beta = 5$, 10, 15 and 20 °C/min. For the fitting we did not use only the two reaction models which are usually used but different kinetic models were used.

In Fig. 10 the results of this fitting for PET containing 2 wt.% OMMT can be seen as an example. The form of the conversion

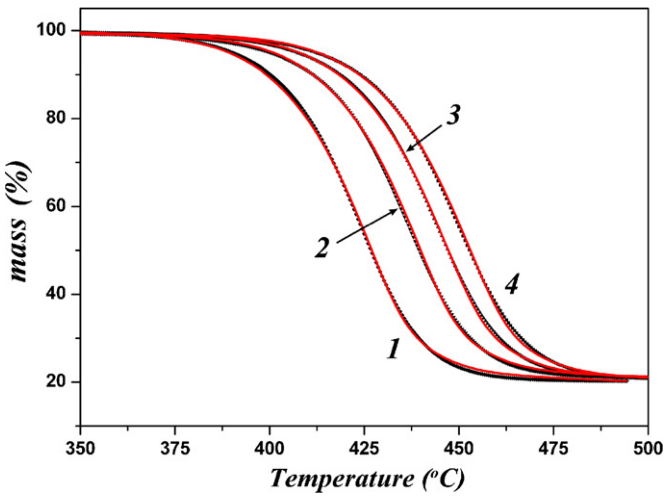

Fig. 10. Fitting (red line) and experimental mass (%) (black symbols) curves for all the different heating rates β for PET containing 2.0 wt.% OMMT. (1) $\beta = 5\,K\,min^{-1}$, (2) $\beta = 10\,K\,min^{-1}$, (3) $\beta = 15\,K\,min^{-1}$, (4) $\beta = 20\,K\,min^{-1}$.

Table 2
Calculated values of activation energy, pre-exponential factor and exponent n for all studied samples.

Samples	$\log A$	E (kJ/mol)	n	$\log K_{cat}$
PET	14.05	223.5	1.51	0.73
PET/OMMT 2 wt.%	14.46	228.3	1.49	0.57
PET/SiO_2 2 wt.%	13.95	222.1	1.62	0.73

function, obtained by fitting, was the mechanism of n^{th}-order auto-catalysis for all the studied samples, that is described by the equation $f(a) = (1-\alpha)^n(1+K_{cat}X)$ where K_{cat} is a constant and X a product in the complex model. The correlation coefficient in all cases was above 0.9999. This model is much more complicated than the n^{th}-order reaction ($f(a) = (1-\alpha)^n$) denting that the decomposition mechanism is a complicated one and for its description must be used not a simple reaction model.

The calculated parameters are presented in Table 2 for all the studied samples. The values of the activation energy were between the limits of the calculated values by the Ozawa method. As can be seen, the fitting to the experimental data was very good for all the range of α. The activation energy of PET was similar to that of its nanocomposite containing fumed silica nanoparticles, while the activation energy of PET containing OMMT was much higher, indicating that OMMT caused a better stabilization effect on the thermal decomposition of PET.

4. Conclusions

The in situ prepared PET nanocomposites showed a fine dispersion of nanoparticles into the polymer matrix. The synthesized organic modifier of montmorillonite based on triphenyphosphine is a thermally stable modifier appropriate for use in the preparation of exfoliated PET/montmorillonite nanocomposites. The used nanoparticles affect directly the molecular weight of PET and cause a substantial enhancement on its tensile strength. Furthermore, both types of nanoparticles act as nucleating agents increasing the crystallization rate of PET since cold-crystallization temperatures sifts to lower values.

From the thermogravimetric curves of PET and its nanocomposites with organically modified montmorillonite and SiO_2 prepared in situ, it was revealed that all samples presented a good thermostability. No remarkable mass loss occurred up until 320–330 °C (<0.4%).

The activation energies for all values of α of neat PET and its nanocomposites were determined using the isoconversional method of Ozawa, Flyn, Wall. It was found that OMMT incurred better thermal stability of PET compared to SiO_2 nanoparticles, since, due to their dispersion in mainly exfoliated form into the PET matrix, much higher surface was available to interact with PET. The degradation mechanism of all studied samples was n^{th}-order auto-catalysis denoting that for a more precise description of the degradation of these nanocomposites, more complicated mechanisms must be used instead of the usually used in the polymers, like the n^{th}-order reaction.

Acknowledgements

This work was funded by the Greek Ministry of Development under the 3th European Community Support Framework, Operational Program “Competiveness” 2000–2006 (PENED, 78108).

References

[1] X. Yao, X. Tian, D. Xie, X. Zhang, K. Zheng, J. Xu, G. Zhang, P. Cui, Interface structure of poly(ethylene terephthalate)/silica nanocomposites, Polymer 50 (2009) 1251–1256.
[2] R.S. Rajeev, E. Harkin-Jones, K. Soon, T. McNally, G. Menary, C.G. Armstrong, P.J. Martin, Studies on the effect of equi-biaxial stretching on the exfoliation of nanoclays in polyethylene terephthalate, Eur. Polym. J. 45 (2009) 332–340.
[3] B.W. Ahn, Y.S. Chi, T.J. Kang, Preparation and characterization of multi-walled carbon nanotube/poly(ethylene terephthalate) nanoweb, J. Appl. Polym. Sci. 110 (2008) 4055–4063.
[4] X. Zhu, B. Wang, S. Chen, C. Wang, Y. Zhang, H. Wang, Synthesis and non-isothermal crystallization behavior of PET/surface-treated TiO_2 nanocomposites, J. Macromol. Sci. Part B: Phys. 47 (2008) 1117–1129.
[5] J. Zheng, P. Cui, X. Tian, K. Zheng, Pyrolysis studies of polyethylene terephthalate/silica nanocomposites, J. Appl. Polym. Sci. 104 (2007) 9–14.
[6] Y. Wang, J. Gao, Y. Ma, U.S. Agarwal, Study on mechanical properties, thermal stability and crystallization behavior of PET/MMT nanocomposites, Composites B 37 (2006) 399–407.
[7] K. Chrissafis, Kinetics of thermal degradation of polymers: complementary use of isoconversional and model-fitting methods, J. Therm. Anal. Calorim. 95 (2009) 273–283.
[8] J. Yang, R. Miranda, C. Roy, Using the DTG curve fitting method to determine the apparent kinetic parameters of thermal decomposition of polymers, Polym. Degrad. Stab. 73 (2001) 455–461.
[9] B.J. Holland, J.N. Hay, The value and limitations of non-isothermal kinetics in the study of polymer degradation, Thermochim. Acta 388 (2002) 253–273.
[10] B. Saha, A.K. Ghoshal, Thermal degradation kinetics of poly(ethylene terephthalate) from waste soft drinks bottles, Chem. Eng. J. 111 (2005) 39–43.
[11] B. Saha, A.K. Maiti, A.K. Ghoshal, Model-free method for isothermal and non-isothermal decomposition kinetics analysis of PET sample, Thermochim. Acta 444 (2006) 46–52.
[12] S. Berkowitz, Viscosity–molecular weight relationships for poly(ethylene terephthalate) in hexafluoroisopropanol-pentafluorophenol using SEC-LALLS, J. Appl. Polym. Sci. 29 (1984) 4353–4361.
[13] A.A. Vassiliou, G.Z. Papageorgiou, D.S. Achilias, D.N. Bikiaris, Non-isothermal crystallisation kinetics of in situ prepared poly(ε-caprolactone)/surface-treated SiO_2 nanocomposites, Macromol. Chem. Phys. 208 (2007) 364–376.
[14] A.A. Vassiliou, D.N. Bikiaris, K. El Mabrouk, M. Kontopoulou, Effect of evolved interactions in poly(butylene succinate)/fumed silica biodegradable in situ prepared nanocomposites on molecular weight, material properties and biodegradability, submitted for publication.
[15] D. Bikiaris, V. Karavelidis, G. Karayannidis, A new approach to prepare poly(ethylene terephthalate)/silica nanocomposites with increased molecular weight and fully adjustable branching or crosslinking by SSP, Macromol. Rapid Commun. 27 (2006) 1199–1205.
[16] F. Wang, X. Meng, X. Xu, B. Wen, Z. Qian, X. Gao, Y. Ding, S. Zhang, M. Yang, Inhibited transesterification of PET/PBT blends filled with silica nanoparticles during melt processing, Polym. Degrad. Stab. 93 (2008) 1397–1404.
[17] S.I. Han, J.S. Lim, D.K. Kim, M.N. Kim, S.S. Im, In situ polymerized poly(butylene succinate)/silica nanocomposites: physical properties and biodegradation, Polym. Degrad. Stab. 93 (2008) 889–895.
[18] D.S. Achilias, D.N. Bikiaris, V. Karavelidis, G.P. Karayannidis, Effect of silica nanoparticles on solid state polymerization of poly(ethylene terephthalate), Eur. Polym. J. 44 (2008) 3096–3107.
[19] K. Chrissafis, G. Antoniadis, K.M. Paraskevopoulos, A. Vassiliou, D.N. Bikiaris, Comparative study of the effect of different nanoparticles on the mechanical properties and thermal degradation mechanism of in situ prepared poly(ε-caprolactone) nanocomposites, Comp. Sci. Technol. 67 (2007) 2165–2174.
[20] D.N. Bikiaris, G.P. Karayannidis, Synthesis and characterisation of branched and partially crosslinked poly(ethylene terephthalate), Polym. Int. 52 (2003) 1230–1239.

[21] T.U. Patro, D.V. Khakhar, A. Misra, Phosphonium-based layered silicate-poly(ethylene terephthalate) nanocomposites: stability, thermal and mechanical properties, J. Appl. Polym. Sci. 11 (2009) 1720–1732.
[22] J. Yang, Y. Lin, J. Wang, M. Lai, J. Li, J. Liu, X. Tong, H. Cheng, Morphology, thermal stability, and dynamic mechanical properties of atactic polypropylene/carbon nanotube composites, J. Appl. Polym. Sci. 98 (2005) 1087–1091.
[23] K. Chrissafis, K.M. Paraskevopoulos, G.Z. Papageorgiou, D.N. Bikiaris, Thermal and dynamic mechanical behavior of bionanocomposites: fumed silica nanoparticles dispersed in poly(vinyl pyrrolidone), chitosan, and poly(vinyl alcohol), J. Appl. Polym. Sci. 110 (2008) 1739–1749.
[24] K. Chen, C.A. Wilkie, S. Vyazovkin, Nanoconfinement revealed in degradation and relaxation studies of two structurally different polystyrene–clay systems, J. Phys. Chem. B 111 (2007) 12685–12692.
[25] G.Z. Papageorgiou, D.S. Achilias, D.N. Bikiaris, G.P. Karayannidis, Isothermal and non-isothermal crystallization kinetics of branched and partially crosslinked PET: DSC study, J. Therm. Anal. Cal. 84 (2006) 85–89.
[26] T.G. Gopakumar, J.A. Lee, M. Kontopoulou, J.S. Parent, Influence of clay exfoliation on the physical properties of montmorillonite/polyethylene composites, Polymer 43 (2002) 5483–5491.
[27] S. Tzavalas, V. Drakonakis, D.E. Mouzakis, D. Fisher, V.G. Gregoriou, Effect of carboxy-functionalized multiwall nanotubes (MWNT–COOH) on the crystallization and chain conformations of poly(ethylene terephthalate) PET in PET–MWNT nanocomposites, Macromolecules 39 (2006) 9150–9156.
[28] G. Antoniadis, K.M. Paraskevopoulos, D. Bikiaris, K. Chrissafis, Kinetics study of cold-crystallization of poly(ethylene terephthalate) nanocomposites with multi-walled carbon nanotubes, Thermochim. Acta 493 (2009) 68–75.
[29] G. Antoniadis, K.M. Paraskevopoulos, D. Bikiaris, K. Chrissafis, Melt-crystallization mechanism of poly(ethylene terephthalate)/multi-walled carbon nanotubes prepared by in situ polymerization, J. Polym. Sci. Part B: Polym. Phys. 47 (2009) 1452–1466.
[30] M. Bailly, M. Kontopoulou, Preparation and characterization of thermoplastic olefin/nanosilica composites using a silane-grafted polypropylene matrix, Polymer 50 (2009) 2472–2480.
[31] W. Xie, Z. Gao, W.P. Pan, D. Hunter, A. Singh, R. Vaia, Thermal degradation chemistry of alkyl quaternary ammonium montmorillonite, Chem. Mater. 13 (2001) 2979–2990.
[32] T. Ozawa, A new method of analyzing thermogravimetric data, Bull. Chem. Soc. Jpn. 38 (1965) 1881–1886.
[33] J. Flynn, L.A. Wall, A quick direct method for determination of activation energy from thermogravimetric data, Polym. Lett. 4 (1966) 323–338.
[34] T. Ozawa, Kinetic analysis of derivative curves in thermal analysis, J. Therm. Anal. 2 (1970) 301–324.
[35] K. Stoeffler, P.G. Lafleur, J. Denault, Thermal decomposition of various alkyl onium organoclays: effect on polyethylene terephthalate nanocomposites' properties, Polym. Degrad. Stab. 93 (2008) 1332–1350.
[36] M.C. Costache, M.J. Heidecker, E. Manias, C.A. Wilkie, Preparation and characterization of poly(ethyleneterephthalate)/clay nanocomposites by melt blending using thermally stable surfactants, Polym. Adv. Technol. 17 (2006) 764–771.
[37] S. Vyazovkin, C.A. Wight, Model-free and model-fitting approaches to kinetic analysis of isothermal and nonisothermal data, Thermochim. Acta 340–341 (1999) 53–68.
[38] S. Vyazovkin, Thermal analysis, Anal. Chem. 80 (2008) 4301–4316.
[39] J.D. Peterson, S. Vyazovkin, C.A. Wight, Kinetics of the thermal and thermo-oxidative degradation of polystyrene, polyethylene and poly(propylene), Macromol. Chem. Phys. 202 (2001) 775–784.
[40] S. Vyazovkin, Modification of the integral isoconversional method to account for variation in the activation energy, J. Comput. Chem. 22 (2001) 178–183.
[41] S. Vyazovkin, N. Sbirrazzuoli, Isoconversional kinetic analysis of thermally stimulated processes in polymers, Macromol. Rapid Commun. 27 (2006) 1515–1532.